

The Decay $Z \rightarrow \bar{\nu}\nu\gamma$ in the Standard Model

J. M. Hernández

Facultad de Ciencias Físico Matemáticas, Universidad Autónoma de Puebla, Apartado Postal 1152, Puebla, México.

M. A. Pérez *, G. Tavares-Velasco and J. J. Toscano † ‡

Departamento de Física, CINVESTAV, Apartado Postal 14-740, 07000, México D. F., México.

(October 25, 2018)

A complete study of the one-loop induced decay $Z \rightarrow \bar{\nu}\nu\gamma$ is presented within the framework of the Standard Model. The advantages of using a nonlinear gauge are stressed. We have found that the main contributions come from the electric dipole and the magnetic dipole transitions of the Z gauge boson and the neutrino, respectively. We obtain a branching ratio $B(Z \rightarrow \bar{\nu}\nu\gamma) = 7.16 \times 10^{-10}$, which is about four orders of magnitude smaller than the bound recently obtained by the L3 Collaboration and thus it leaves open a window to search for new physics effects in single-photon decays of the Z boson.

14.70Hp, 13.38Dg, 13.15+g, 12.15.L.k

I. INTRODUCTION

In the absence of any clear deviation from the Standard Model (SM) predictions, considerable work has been done recently to search for processes that are forbidden or highly suppressed and may become a good playground to test any new physics lying beyond the SM. The radiative decay $Z \rightarrow \bar{\nu}\nu\gamma$ is a good example of this type of processes because it arises at the one-loop level in the SM. The L3 Collaboration has searched for energetic photon events coming from single-photon Z decays. It was obtained a bound of one part in a million for the respective branching ratio [1]. Single photon events in Z decays have been associated to gauge boson and leptonic substructure [2,3], supersymmetric particles [4], a possible neutrino magnetic moment [5] and the production of a Higgs boson with its associated CP-odd majoron [6]. The decay $Z \rightarrow \bar{\nu}\nu\gamma$ is expected also to be sensitive to the possible anomalous electromagnetic properties of the Z boson and the neutrinos. The latter point has become of increased interest after the recent evidence of oscillations in atmospheric neutrinos [7]. In a recent study of the decay $Z \rightarrow \bar{\nu}\nu\gamma$ within the effective Lagrangian approach [8,9], the L3 bound was used to get direct constraints on dimension-six and dimension-eight operators associated with the anomalous electromagnetic properties of the neutrino.

Though there is a great incentive in studying single-photon Z decays, to our knowledge its decay width has not been computed in the SM. We would like to stress that in order to disentangle new contributions to this process, it is important to count with a complete analysis of the SM contributions. Our general aim is precisely to present explicit expressions of a calculation of the SM decay $Z \rightarrow \bar{\nu}\nu\gamma$ at lowest order in perturbation theory. As we will see below, the amplitude for this process can be written in terms of five independent $U_e(1)$ gauge structures. Some of them can be identified in terms of the so-called off-shell electromagnetic properties of the Z gauge boson and the neutrino. It is well known that the Z boson possesses both an anapole moment (AM) and an electric dipole transition (EDT) defined through the $ZZ\gamma^*$ and $ZZ^*\gamma$ couplings, respectively (where $*$ stands for off-shell particles) [2]. A SM neutrino can have only off-shell electromagnetic properties characterized by the $\nu\nu\gamma^*$ and $\nu\nu^*\gamma$ couplings. The $\nu\nu\gamma^*$ coupling corresponds to an AM of the neutrino, which has been extensively studied in the literature [10,11]. It will be seen below that the $\nu\nu^*\gamma$ coupling can be identified with a magnetic dipole transition (MDT) of the neutrino. In this paper we have found that the main contributions to the decay $Z \rightarrow \bar{\nu}\nu\gamma$ come precisely from the MDT and EDT properties of the neutrino and the Z boson, respectively. In particular, the MDT of the neutrino plays an important role in this process. Therefore, we will discuss with some extent its $SU(2)$ structure. For this purpose we will use

*E-mail: mperez@fis.cinvestav.mx

†On leave from Facultad de Ciencias Físico Matemáticas, Universidad Autónoma de Puebla.

‡E-mail: jtoscana@fcfm.buap.mx

a nonlinear gauge which allows us to separate in a transparent way the $SU(2)$ and $U_e(1)$ gauge structures and, as a consequence, it will simplify considerably the calculation. In particular, we have found that there is no $SU(2)$ gauge link between the $\nu\nu^*\gamma$ coupling and the box diagrams contributing to the decay. This result should be contrasted with the situation found in the calculation of the SM scattering amplitude of neutrinos with charged leptons and nucleons. In this case, the $SU(2)$ gauge structure of the $\nu\nu\gamma^*$ coupling is directly linked to the box diagrams contributing to the scattering process [10].

In the nonlinear gauge the decay $Z \rightarrow \bar{\nu}\nu\gamma$ receives contributions from reducible triangle diagrams characterized by the $ZZ^*\gamma$ and $\nu\nu^*\gamma$ couplings, as well as from box diagrams containing W boson and lepton combined effects. It is well known that in many four-body processes the box diagrams contributions can be neglected compared with the triangle ones. However, this approximation fails when the triangle and box diagrams possess common $U_e(1)$ gauge structures which induce form factors of the same order of magnitude. In particular, the tensor structures arising from the box diagrams will have a Lorentz covariant decomposition inducing the MDT of the neutrino. Therefore, it is not possible to neglect the box diagram contributions in the decay $Z \rightarrow \bar{\nu}\nu\gamma$. Our numerical result confirms that this decay is a SM highly suppressed process, about four orders of magnitude below the L3 bound [1]. Thus it leaves open a window to search for new physics effects in single-photon events, mainly in the neutrino sector.

We have organized our presentation in the following way. In Sec. II we present the analytic expressions for the $Z \rightarrow \bar{\nu}\nu\gamma$ decay width. In Sec. III we give details of the numerical analysis, and the conclusions are presented in Sec. IV.

II. THE NONLINEAR GAUGE AND THE DECAY $Z \rightarrow \bar{\nu}\nu\gamma$

The decay $Z \rightarrow \bar{\nu}\nu\gamma$ is a SM one-loop prediction which receives contributions from all charged particles. Within the conventional linear gauge, we can classify in five sets the Feynman diagrams contributing to this decay at the one-loop level. The first three sets are characterized by reducible diagrams including the $Z^* - \gamma$ mixing term (Fig. 1) and the $ZZ^*\gamma$ and $\nu\nu^*\gamma$ couplings (Fig. 2 and Fig. 3, respectively), while the other two sets include box diagrams where the Z boson couples to charged leptons (Fig. 4) and to W bosons (Fig. 5). For the purpose of our calculation, it is suitable using a nonlinear gauge in which there is no $SU(2)$ gauge (nor $U_e(1)$ gauge) link between the $\nu\nu^*\gamma$ coupling and the box diagrams. This task is a difficult one to fulfill in a linear gauge, where $SU(2)$ gauge independence and $U_e(1)$ gauge invariance are only accomplished after adding up almost all the Feynman diagrams involved in the calculation. Furthermore, in this type of gauges a renormalization of the $Z^* - \gamma$ mixing term has to be done [12]. In contrast, it can be shown that in the nonlinear gauge the amplitude for this mixing term vanishes for any value of the $SU(2)$ gauge parameter ξ . We will show also that the $\nu\nu^*\gamma$ coupling is by itself $SU(2)$ gauge independent and $U_e(1)$ gauge invariant.

A nonlinear R_ξ -gauge condition was first introduced by Fujikawa [13]. The ordinary derivative involved in the gauge-fixing term for the W boson is replaced by the respective $U_e(1)$ covariant derivative; as a consequence, there are no $W^\pm G^\mp \gamma$ unphysical vertices, with G^\pm the respective would-be Goldstone boson. The W boson and the charged ghosts sectors are separately $U_e(1)$ gauge invariant, leading to naive Ward identities. This procedure was later extended to remove both $W^\pm G^\mp \gamma$ and $W^\pm G^\mp Z$ vertices [14,15]. It is possible to proceed further with this scheme and remove more unphysical vertices, such as $H^0 W^\pm G^\mp \gamma(Z)$ and $G^0 W^\pm G^\mp \gamma(Z)$, with G^0 and H^0 the neutral would-be Goldstone and physical Higgs bosons, respectively [16,17]. For our present purposes, we will use a gauge-fixing functional which is nonlinear in the vector sector but linear in the scalar sector.

The functionals which define the respective W , Z and A propagators in the nonlinear gauge can be written as

$$\begin{aligned} f^+ &= \bar{D}_\mu W^{+\mu} - i\xi m_W G^+, \\ f^Z &= \partial_\mu Z^\mu - \xi m_Z G^0, \\ f^A &= \partial_\mu A^\mu, \end{aligned} \tag{1}$$

where $s_w = \sin\theta_w$, $c_w = \cos\theta_w$ and θ_w is the weak mixing angle. We have also defined the following operator

$$\bar{D}_\mu = \partial_\mu - ig' B_\mu, \tag{2}$$

$Z_\mu = c_w W_\mu^3 - s_w B_\mu$, $A_\mu = s_w W_\mu^3 + c_w B_\mu$, and W_μ^i and B_μ are the gauge fields of the SU(2) and U_Y(1) groups, respectively. We can see that the above operator contains the electromagnetic covariant derivative, so that the f^\pm functionals transform covariantly under the U_e(1) group. The corresponding gauge fixing Lagrangian is given by

$$\mathcal{L}_{GF} = -\frac{1}{\xi} f^+ f^- - \frac{1}{2\xi} (f^Z)^2 - \frac{1}{2\xi} (f^A)^2, \quad (3)$$

which removes the $W^\pm G^\mp \gamma$ and $W^\pm G^\mp Z$ vertices from the Higgs kinetic energy term $(D_\mu \phi)^\dagger (D^\mu \phi)$. The corresponding Faddeev–Popov Lagrangian is given by

$$\begin{aligned} \mathcal{L}_{FP} = & -\bar{c}^- [\bar{D}_\mu \hat{D}^\mu + \xi m_W (m_W + H^0 + iG^0)] c^+ - ig c_w \bar{c}^- \bar{D}_\mu (W^{+\mu} c_Z) - ie \bar{c}^- \bar{D}_\mu (W^{+\mu} c_\gamma) \\ & - i \frac{g s_w^2}{c_w} W^{+\mu} \bar{c}^- (\partial^\mu c_Z) + ie W_\mu^+ \bar{c}^- (\partial^\mu c_\gamma) - ig c_w W^{+\mu} (\partial_\mu \bar{c}_Z) c^- - ie W^{+\mu} (\partial_\mu \bar{c}_\gamma) c^- \\ & - g c_{2w} m_Z \xi (G^+ \bar{c}^- c_Z + G^+ \bar{c}_Z c^-) - e m_W \xi (G^+ \bar{c}^- c_\gamma + G^+ \bar{c}_\gamma c^-) + H.C. \\ & - \bar{c}_Z [\square + \xi m_Z (m_Z + H^0)] c_Z - \bar{c}_\gamma \square c_\gamma, \end{aligned} \quad (4)$$

where $\bar{c}^\pm (c^\pm)$, $\bar{c}_Z (c_Z)$, and $\bar{c}_\gamma (c_\gamma)$ are the pairs of ghosts associated with the W^\pm , Z , and A gauge bosons, respectively, and $c_{2w} = c_w^2 - s_w^2$. The charged ghosts satisfy $(\bar{c}^+)^\dagger = \bar{c}^-$ and $(c^+)^\dagger = c^-$. We have introduced the following operator

$$\hat{D}_\mu = \partial_\mu - ig W_\mu^3, \quad (5)$$

which also contains the electromagnetic covariant derivative¹. Therefore, just as it was the case with the $f^- f^+$ term in \mathcal{L}_{GF} , the \mathcal{L}_{FP} Lagrangian is invariant under the U_e(1) group. Since both the Yang–Mills and the kinetic energy Higgs sectors can be expressed in terms of the \bar{D}_μ and \hat{D}_μ operators, all the charged sector of the SM satisfies naive Ward identities.

To calculate the amplitude for the decay $Z \rightarrow \bar{\nu} \nu \gamma$ in the nonlinear gauge, the Feynman rules for the $A_\lambda(k_1) W_\rho^+(k_2) W_\eta^-(k_3)$, $Z_\lambda(k_1) W_\rho^+(k_2) W_\eta^-(k_3)$, and $A_\rho Z_\lambda W_\alpha^+ W_\beta^-$ vertices are required

$$\begin{aligned} \Gamma_{\lambda\rho\eta}^{AWW} &= -ie[(k_3 - k_1 + \frac{k_2}{\xi})_\rho g_{\lambda\eta} + (k_1 - k_2 - \frac{k_3}{\xi})_\eta g_{\lambda\rho} + (k_2 - k_3)_\lambda g_{\rho\eta}], \\ \Gamma_{\lambda\rho\eta}^{ZWW} &= -ig c_w[(k_3 - k_1 - \frac{s_w^2 k_2}{c_w^2 \xi})_\rho g_{\lambda\eta} + (k_1 - k_2 + \frac{s_w^2 k_3}{c_w^2 \xi})_\eta g_{\lambda\rho} + (k_2 - k_3)_\lambda g_{\rho\eta}], \\ \Gamma_{\rho\lambda\alpha\beta}^{AZWW} &= -ie g c_w [2g_{\alpha\beta} g_{\rho\lambda} - (1 + \frac{1}{\xi} \frac{s_w^2}{c_w^2})(g_{\alpha\lambda} g_{\beta\rho} + g_{\beta\lambda} g_{\alpha\rho})], \end{aligned} \quad (6)$$

where all the momenta are incoming. We have taken the lepton masses to be zero except where large logs (collinear singularities) arise. This approximation and the use of the nonlinear gauge reduce considerably the number of diagrams involved in the calculation. We have calculated the Feynman amplitudes using the computer program FeynCalc [19].

In the linear gauge the $Z^* - \gamma$ mixing term receives contributions from W^\pm gauge bosons, charged ghosts and $W^\pm G^\mp$ combined effects². In contrast, in the nonlinear gauge the $W^\pm G^\mp$ combined effects are absent. From (1), (3) and (4) we can see that the $f^+ f^-$ term in the \mathcal{L}_{GF} and the \mathcal{L}_{FP} Lagrangians also presents explicit U_e(1) gauge invariance. Consequently, in this gauge we expect a zero contribution arising from all charged particles. This fact was shown before in the Feynman–t’Hooft version of the nonlinear gauge [17,18]. We will show that this result is valid for any value of the gauge parameter ξ . Notice that the charged part of the \mathcal{L}_{FP} Lagrangian resembles scalar electrodynamics (see (4)), so that we do not expect anything new coming from these particles in the general nonlinear

¹Notice that if we use in (1) \hat{D}_μ instead of \bar{D}_μ , as it was pointed out in [18], the $W^\pm G^\mp \gamma$ vertex is removed but the $W^\pm G^\mp Z$ vertex only becomes modified.

²Since the Lagrangian which defines the G^\pm boson is not modified in its interactions with the photon by the gauge fixing procedure used for the SU(2) group, and since it resembles scalar electrodynamics, the contribution of this field to the $Z^* - \gamma$ mixing term vanishes in any gauge.

R_ξ -gauge. In contrast, both the W -propagator and the $W^\pm W^\mp \gamma(Z)$ vertices have a nontrivial dependence on the ξ parameter. The corresponding amplitude which arises from the diagrams shown in Figs. 1(a) and 1(b) is given by

$$\Pi_{\alpha\beta}^{Z^*\gamma} = \frac{ieg c_w m_W^2}{64\pi^2} [U_a + U_b + \frac{s_w^2}{c_w^2} (V_a + V_b)] g_{\alpha\beta}, \quad (7)$$

with $U_a(U_b)$ and $V_a(V_b)$ characterizing the loops in Figs. 1(a) (1(b)). After a straightforward calculation, we have found that there is not $Z^* - \gamma$ mixing term in the general nonlinear R_ξ -gauge

$$\begin{aligned} U_a &= -U_b = \xi^2 [5 + 6B_0(0, \xi m_W^2, \xi m_W^2)] - 3[1 + 6B_0(0, m_W^2, m_W^2)], \\ V_a &= -V_b = -\xi [3 + 2B_0(0, \xi m_W^2, \xi m_W^2)] - \frac{1}{\xi} [5 + 6B_0(0, m_W^2, m_W^2)], \end{aligned} \quad (8)$$

where $B_0(0, \xi m_W^2, \xi m_W^2)$ and $B_0(0, m_W^2, m_W^2)$ are Passarino-Veltman two-point scalar functions [20].

In this manner, the width for the decay $Z \rightarrow \bar{\nu}\nu\gamma$ can be expressed as

$$\Gamma(Z \rightarrow \bar{\nu}\nu\gamma) = \frac{m_Z}{256\pi^3} \int_0^1 dx \int_0^{1-x} dy |\mathcal{M}|^2, \quad (9)$$

where \mathcal{M} is the invariant amplitude

$$\mathcal{M} = \bar{u}_L(p_1) [\mathcal{M}_{Z^*}^{\alpha\beta} + \mathcal{M}_{\nu^*}^{\alpha\beta} + \mathcal{M}_{Box4}^{\alpha\beta} + \mathcal{M}_{Box5}^{\alpha\beta}] v_R(p_2) \epsilon_\alpha(k_2, \lambda_2) \epsilon_\beta^*(k_1, \lambda_1), \quad (10)$$

and the $\mathcal{M}_{Z^*}^{\alpha\beta}$, $\mathcal{M}_{\nu^*}^{\alpha\beta}$, $\mathcal{M}_{Box4}^{\alpha\beta}$, $\mathcal{M}_{Box5}^{\alpha\beta}$ amplitudes correspond to the respective diagrams shown in Figs. 2–5. The explicit form of these amplitudes will be given below. Moreover, $p_1(p_2)$ are the neutrino(antineutrino) momenta, $k_1(k_2)$ are the $\gamma(Z)$ momenta, $\epsilon_\beta(\epsilon_\alpha)$ are the $\gamma(Z)$ polarization vectors, and $u_L = \frac{1}{2}(1 - \gamma_5)u$. It is useful to define the following dimensionless quantities

$$x = \frac{2k_1 \cdot p_1}{m_Z^2}, \quad y = \frac{2k_1 \cdot p_2}{m_Z^2}. \quad (11)$$

and the combinations $\delta = 1 - x - y$, $\delta_+ = x + y$, $\delta_- = x - y$, $\delta_x = 1 - x$, $\delta_y = 1 - y$.

A. $ZZ^*\gamma$ coupling contribution

The $ZZ^*\gamma$ coupling contributes to the decay $Z \rightarrow \bar{\nu}\nu\gamma$ through the reducible diagram shown in Fig. 2. The contributions to this coupling are due to the fermion triangle diagram responsible for the ABJ anomaly, which of course vanishes with the SM fermion multiplet assignment. The corresponding amplitude must be $U_e(1)$ gauge invariant by itself. This amplitude was obtained by Barroso et al. some time ago [2]. We have reproduced this result to compute the corresponding contribution to the decay $Z \rightarrow \bar{\nu}\nu\gamma$. Since one Z boson and the photon are on-shell, we take $k_1^\beta \epsilon_\beta = k_2^\alpha \epsilon_\alpha = 0$, $k_1^2 = 0$, $k_2^2 = m_Z^2$. In addition, using Bose statistics and the Ward identity satisfied by the electromagnetic current, we obtain for this amplitude

$$\begin{aligned} G^{\alpha\beta\gamma} &= \frac{ig^2 e}{2c_w^2 \pi^2} \sum_f g_V^f g_A^f Q_f \left\{ \frac{1}{q^2 - m_Z^2} [m_f^2 C_0(m_Z^2, q^2) \right. \\ &\quad - \frac{m_Z^2}{2(q^2 - m_Z^2)} (B_0(m_Z^2) - B_0(q^2)) + \frac{1}{2} \epsilon^{\alpha\beta\lambda\rho} k_{2\lambda} q_\rho q^\gamma \\ &\quad \left. + \frac{1}{2} \frac{q^2 + m_Z^2}{q^2 - m_Z^2} [m_f^2 C_0(m_Z^2, q^2) - \frac{q^2 m_Z^2}{q^4 - m_Z^4} (B_0(m_Z^2) - B_0(q^2)) + \frac{1}{2} \epsilon^{\alpha\beta\gamma\lambda} k_{1\lambda}] \right\}, \end{aligned} \quad (12)$$

where $C_0(m_Z^2, q^2) = C_0(0, m_Z^2, q^2, m_f^2, m_f^2, m_f^2)$, $B_0(m_Z^2) = B_0(m_Z^2, m_f^2, m_f^2)$, and $B_0(q^2) = B_0(q^2, m_f^2, m_f^2)$ are Passarino-Veltman three- and two-point scalar functions written in the notation of [19]. Q_f is the electric charge in units of e , $q^2 = (p_1 + p_2)^2 = m_Z^2 \delta$, $g_V^f = t_3^f - 2Q_f s_w^2$, and $g_A^f = t_3^f$, with t_3^f the third component of weak isospin.

Now, it is straightforward to obtain the respective contribution to the decay $Z \rightarrow \bar{\nu}\nu\gamma$

$$\mathcal{M}_{Z^*}^{\alpha\beta} = \frac{2i\alpha^2}{(s_w c_w)^3} \gamma_\lambda \sum_f g_V^f g_A^f Q^f F(m_Z^2, q^2, m_f^2) \epsilon^{\alpha\beta\lambda\rho} k_{1\rho}, \quad (13)$$

where

$$F(m_Z^2, q^2, m_f^2) = \frac{1}{(q^2 - m_Z^2)^2} [(q^2 + m_Z^2) m_f^2 C_0(m_Z^2, q^2) - \frac{q^2 m_Z^2}{q^2 - m_Z^2} (B_0(m_Z^2) - B_0(q^2))]. \quad (14)$$

In addition, we have removed from (14) the mass independent term which vanish when we perform the summation over fermion families.

As it was shown in [2], and more recently in [21], the Z boson possesses only off-shell electromagnetic properties characterized by an electric dipole transition (EDT) and an anapole moment (AM), which correspond to the $ZZ^*\gamma$ and $ZZ\gamma^*$ couplings, respectively. Since the on-shell $ZZ\gamma$ vertex is zero, the Z boson does not possess on-shell (physical) electromagnetic properties. So the contribution of the $ZZ^*\gamma$ coupling to the decay $Z \rightarrow \bar{\nu}\nu\gamma$ corresponds to an EDT, which is a transfer-momentum dependent quantity. This EDT electromagnetic property of the Z boson depends only on the number of families. Indeed, as we will discuss in the following section, the contributions arising from the first two families, which are nearly mass degenerated, are very small compared with the corresponding contribution of the third family, where the masses involved have an important gap.

B. $\nu\nu^*\gamma$ coupling contribution

The decay $Z \rightarrow \bar{\nu}\nu\gamma$ receives contributions coming from the $\nu\nu^*\gamma$ coupling through the diagrams shown in Figs. 3(a) and 3(b), where the photon couples to leptons and to W bosons, respectively. We will present the calculation for the $\nu\nu^*\gamma$ coupling in the general nonlinear R_ξ -gauge and then we will use it to give the corresponding amplitude for the decay $Z \rightarrow \bar{\nu}\nu\gamma$. The triangle 3(a) depends on the gauge parameter ξ only through the W -propagator. On the other hand, the triangle 3(b) has a more complicated ξ dependence through both the W -propagator and the $W^\pm W^\mp \gamma$ vertex. Taking into account that a neutrino and the photon are on-shell, the amplitude for the $\nu\nu^*\gamma$ coupling can be written as

$$\Gamma_{\beta}^{\nu\nu^*\gamma} = \frac{ig^2 e}{16\pi^2} \frac{1}{p^2} \left[\frac{p^2}{2} \gamma_{\beta} (F_a + F_b) + p_{1\beta} \not{k}_1 (G_a + G_b) \right], \quad (15)$$

where $p^2 = (k_1 + p_1)^2 = xm_Z^2$ is the momentum transferred by the Z boson. $F_a(F_b)$ and $G_a(G_b)$ are the amplitudes corresponding to diagrams 3(a) (3(b))

$$\begin{aligned} F_a &= \frac{m_W^2}{p^2} + \frac{1}{2}(1 - \xi) + \frac{1}{2}\left(1 - \frac{2m_W^2}{p^2}\right)\left(1 - \frac{p^2}{m_W^2}\right)B_0(p^2, 0, m_W^2) \\ &\quad - \frac{\xi}{2}B_0(0, \xi m_W^2, \xi m_W^2) + \frac{1}{2}\left(\frac{p^2}{m_W^2} - \xi\right)B_0(p^2, 0, \xi m_W^2) \\ &\quad - \left(\frac{3}{2} - \frac{m_W^2}{p^2}\right)B_0(0, m_W^2, m_W^2), \end{aligned} \quad (16)$$

$$G_a = 1 - \frac{2m_W^2}{p^2} - 2\left(1 - \frac{m_W^2}{p^2}\right)[B_0(p^2, 0, m_W^2) - B_0(0, m_W^2, m_W^2)], \quad (17)$$

$$\begin{aligned} F_b &= 2 - \frac{m_W^2}{p^2} - \frac{1}{2}(1 - \xi) - \frac{1}{2}\left(1 - \frac{2m_W^2}{p^2}\right)\left(1 - \frac{p^2}{m_W^2}\right)B_0(p^2, 0, m_W^2) + \frac{1}{2}\xi B_0(0, \xi m_W^2, \xi m_W^2) \\ &\quad - \frac{1}{2}\left(\frac{p^2}{m_W^2} - \xi\right)B_0(p^2, 0, \xi m_W^2) + \left(\frac{3}{2} - \frac{m_W^2}{p^2}\right)B_0(0, m_W^2, m_W^2) + 2(m_W^2 - p^2)C_0(3), \end{aligned} \quad (18)$$

$$G_b = -3 + \frac{2m_W^2}{p^2} + 2(1 - \frac{m_W^2}{p^2})[B_0(p^2, 0, m_W^2) - B_0(0, m_W^2, m_W^2)] - 2(m_W^2 - p^2)C_0(3), \quad (19)$$

where the three-point scalar function is defined in the Appendix. From (15)–(19) it is evident that the amplitude for the $\nu\nu^*\gamma$ coupling is a SU(2) gauge independent and U_e(1) gauge invariant quantity that can be written as

$$\Gamma_{\beta}^{\nu\nu^*\gamma} = i \frac{A(p^2)}{p^2} k_1^{\mu} \sigma_{\mu\beta} \not{p}, \quad (20)$$

where $\sigma_{\mu\beta} = \frac{i}{2}(\gamma_{\mu}\gamma_{\beta} - \gamma_{\beta}\gamma_{\mu})$, and

$$A(p^2) = \frac{g^2 e}{16\pi^2} [1 + (m_W^2 - p^2)C_0(3)]. \quad (21)$$

It is well known that in the SM the neutrino have no static electromagnetic properties. It is easy to see that our result (21) is consistent with this fact by noting that the $A(p^2)$ form factor vanishes when the neutrino is on-shell. Using the above results, it is straightforward to calculate the corresponding amplitude for the decay $Z \rightarrow \bar{\nu}\nu\gamma$. Taking into account all diagrams shown in Fig. 3, we have

$$\mathcal{M}_{\nu^*}^{\alpha\beta} = \frac{\alpha^2}{2c_w s_w^3 m_Z^2} [A_1(x)\Gamma_1^{\alpha\beta} + A_2(y)\Gamma_2^{\alpha\beta}], \quad (22)$$

where the form factors $A_1(x)$ and $A_2(y)$ are transfer-momentum dependent quantities given by

$$A_1(x) = \frac{1}{x} [1 + m_Z^2(c_w^2 - x)C_0(3)], \quad A_2(y) = A_1(x \rightarrow y). \quad (23)$$

and the U_e(1) gauge structures are given by

$$\Gamma_1^{\alpha\beta} = i k_{1\mu} \sigma^{\beta\mu} \gamma^{\alpha}, \quad \Gamma_2^{\alpha\beta} = i k_{1\mu} \gamma^{\alpha} \sigma^{\mu\beta}. \quad (24)$$

The $\mathcal{M}_{\nu^*}^{\alpha\beta}$ amplitude can be interpreted in terms of the off-shell electromagnetic properties of the neutrino. In fact, we can identify in the gauge structure of this amplitude the familiar form of a fermionic magnetic dipole transition. Since the corresponding form factor is an on-shell vanishing quantity, we can relate it with a MDT of the neutrino. We would like also to stress an aspect related with the off-shell electromagnetic properties of the neutrino, namely, the MDT an AM. We have found that the MDT is an SU(2) gauge independent and U_e(1) gauge invariant quantity. This result must be contrasted with the one obtained for the AM arising from the $\bar{\nu}\nu\gamma^*$ coupling which depends on the gauge parameter ξ [10,11].

C. Box diagrams contribution

In this section we present the amplitudes for the box diagrams contributing to the decay $Z \rightarrow \bar{\nu}\nu\gamma$. These diagrams, shown in Figs. 4 and 5, induce terms with the same Lorentz structure of the neutrino MDT. This implies that we can not neglect these contributions because they are of the same order of magnitude than the one induced by the $\nu\nu^*\gamma$ coupling. We have found that there is not $Z^* - \gamma$ mixing term in the general nonlinear R_{ξ} -gauge. Also, we have found that the $\nu\nu^*\gamma$ coupling is SU(2) gauge independent and U_e(1) gauge invariant. This implies that the contributions arising from the box diagrams must respect these properties by themselves. Even more, since the two sets of box diagrams arise from different Z boson couplings, we expect that they are separately SU(2) gauge independent and U_e(1) gauge invariant. We have found that in the Feynman-t'Hooft version of the nonlinear R_{ξ} -gauge the respective amplitude is U_e(1) invariant and finite for each set of diagrams

$$\mathcal{M}_{Box4}^{\alpha\beta} = \frac{\alpha^2 c_{2w}}{2c_w s_w^3 m_Z^2} \sum_{i=1}^7 A_i^l(x, y) \Gamma_i^{\alpha\beta} \quad (25)$$

and

$$\mathcal{M}_{Box5}^{\alpha\beta} = \frac{\alpha^2 c_w}{s_w^3 m_Z^2} \sum_{i=1}^7 A_i^W(x, y) \Gamma_i^{\alpha\beta}, \quad (26)$$

where the $\Gamma_1^{\alpha\beta}$ and $\Gamma_2^{\alpha\beta}$ $U_e(1)$ gauge structures are given in (24) and

$$\begin{aligned} \Gamma_3^{\alpha\beta} &= \frac{1}{m_Z^2} \gamma^\alpha (k_1 \cdot p_1 p_2^\beta - k_1 \cdot p_2 p_1^\beta), \\ \Gamma_4^{\alpha\beta} &= \frac{1}{m_Z^2} \gamma_\mu p_1^\alpha (k_1 \cdot p_1 g^{\mu\beta} - k_1^\mu p_1^\beta), \quad \Gamma_6^{\alpha\beta} = \Gamma_4^{\alpha\beta} (p_1 \leftrightarrow p_2), \\ \Gamma_5^{\alpha\beta} &= \frac{1}{m_Z^2} \gamma_\mu p_2^\alpha (k_1 \cdot p_1 g^{\mu\beta} - k_1^\mu p_1^\beta), \quad \Gamma_7^{\alpha\beta} = \Gamma_5^{\alpha\beta} (p_1 \leftrightarrow p_2), \end{aligned} \quad (27)$$

while the A_i^l and A_i^W functions are given by

$$\begin{aligned} A_1^l(x, y) &= \frac{1}{2xy\delta_+} \{ \delta_- [B_0(5) - B_0(6)] - x\delta_+ [B_0(6) - B_0(1)] - y[B_0(6) - B_0(2)] \} \\ &+ \frac{m_Z^2}{4\delta x^2 y^2} \{ \delta_- \delta_+ [x(x + 2\delta_y)y^2 + 2xy(1 + x)c_w^2 + \delta_- \delta_+ c_w^4] C_0(3) \\ &+ y\delta [x(5x + 2\delta_y)y^2 + 2xy(2\delta_+ - \delta_x)c_w^2 + \delta_- \delta_+ c_w^4] C_0(4) \\ &+ x[x\delta(x\delta - 2y^2) - 2x(x - \delta_- \delta_+)c_w^2 - \delta_- \delta_+ c_w^4] C_0(7) \\ &+ y[\delta^2 y^2 - 2y(x\delta_x + y\delta_y)c_w^2 - \delta_- \delta_+ c_w^4] C_0(8) \\ &+ x[y\delta_x(\delta_x^2 + 2(\delta_x + 2y)) + 2(\delta_x^2 + xy\delta - y\delta_y)c_w^2] C_0(9) \\ &+ y\delta_y[y\delta_y(4x - \delta_y) + 2(x - y\delta_y)c_w^2] C_0(10) + \delta^2 [\delta\delta_- \delta_+ + 2xy^2 + \delta_- \delta_+ c_w^2] C_0(11) \} \\ &+ \frac{m_Z^4}{4\delta x^2 y^2} \{ [(x + 2\delta_y)x^2 y^3 - xy^2(x(3\delta + 10) - 2y\delta_y)c_w^2 + xy(\delta^2 + 2x(1 + 3y) + 4\delta_y)c_w^4 \\ &- \delta_- \delta_+ c_w^6] D_0(4) + (x\delta + \delta_+ c_w^2)[x\delta(x\delta - 2y^2) + 2x(x - \delta_- \delta_+)c_w^2 + \delta_- \delta_+ c_w^4] D_0(5) \\ &- (y\delta + \delta_+ c_w^2)[y^2\delta^2 - 2y(\delta_+^2 - y)c_w^2 + \delta_- \delta_+ c_w^4] D_0(6) \}, \end{aligned} \quad (28)$$

$$A_2^l(x, y) = -A_1^l(x \leftrightarrow y), \quad (29)$$

$$\begin{aligned} A_3^l(x, y) &= \frac{1}{2xy\delta} \{ [B_0(6) - B_0(5)] + 2xy[B_0(1) - B_0(6)] \} \\ &+ \frac{m_Z^2}{2x^2 y^2 \delta^2} \{ x[xy(3xy + 2\delta^2) + 4xy c_w^2 + \delta_+^2 c_w^2] C_0(3) \\ &+ x[x(x + 2y)\delta^2 - 2x(x^2 + y(y - 2\delta_+))c_w^2 + \delta_+^2 c_w^4] C_0(7) \\ &- x[x^2(3y^2\delta_x + y^3) + 2x(y^2 + x\delta^2)] C_0(9) + x^2\delta^2(\delta + 2c_w^2) C_0(11) \} \\ &+ \frac{m_Z^4}{2x^2 y^2 \delta^2} \{ \frac{1}{2}xy(\delta^2 - 3xy) + (2x^2(x - 2) + xy + \frac{1}{2}\delta(2 + 3xy))c_w^2 + \frac{1}{2}\delta(\delta - 6)c_w^4 \} D_0(4) \\ &- (x\delta + \delta_+ c_w^2)[x\delta^2(x + 2y) + 2x(\delta_x(x + 2y) - y^2)c_w^2 + \delta_+^2 c_w^4] D_0(5) \} + (x \leftrightarrow y), \end{aligned} \quad (30)$$

$$\begin{aligned} A_4^l(x, y) &= \frac{2}{x\delta_+} + \frac{2}{x^2\delta_y\delta_+^2} \{ (2x + y)[B_0(5) - B_0(6) + y(B_0(6) - B_0(2))] + x^2[B_0(5) - B_0(2)] \} \\ &+ \frac{m_Z^2}{x^3 y \delta^2} \{ x[x(x^2\delta - 2\delta^2) + yc_w^2] C_0(3) + y(x\delta_x^2 + yc_w^2) C_0(4) \\ &+ xy c_w^4 C_0(7) + y^2(\delta + c_w)^2 C_0(8) - x\delta_x^3 c_w^2 C_0(9) \\ &+ [-y\delta_y\delta^2 + \delta_y(x - 2\delta_- \delta_+ + 2y\delta_x)c_w^2 + \frac{x^3}{\delta_y}(y(2 + y) - 1)c_w^2] C_0(10) \\ &+ y\delta^2(\delta + 2c_w^2) C_0(11) \} \\ &+ \frac{m_Z^4}{x^3 y \delta^2} \{ [x^2 y \delta_x^2 - x(x\delta_x^2 + xy(2 + x) - y(3 - y))c_w^2 + y\delta_+ c_w^4] D_0(4) \\ &+ y(x\delta + \delta_+ c_w^2)[x(x + 2y)\delta^2 + 2x(\delta_x(x + 2y) - y^2)c_w^2 + \delta_+^2 c_w^4] D_0(5) + y(y\delta + \delta_+ c_w^2)(\delta + c_w^2)^2 D_0(6) \}, \end{aligned} \quad (31)$$

$$\begin{aligned}
A_5^l(x, y) = & \frac{2}{x\delta_+} + \frac{1}{x^2y\delta^2\delta_+^2}\{[y\delta_+(x-2\delta_y) - xy\delta + x^2\delta_+][B_0(6) - B_0(5)] + x^2\delta_+^2[B_0(6) - B_0(1)] \\
& + y\delta_+^2(x-2\delta_y)[B_0(2) - B_0(6)]\} \\
& + \frac{m_Z^2}{2x^3y^2\delta^2}\{[x(-3x^2y^2 - 2xy(x(2x+\delta_x)) - \delta)c_w^2 - (x\delta_-\delta_+ + 2y^2\delta)c_w^4]C_0(3) \\
& - [3x^3y^2 + 2xy(\delta\delta_x + 2x^2)c_w^2 + (x\delta_-\delta_+ + 2y^2\delta)c_w^4]C_0(4) \\
& + x[-x^3\delta^2 + 2x(x(\delta_-\delta_+ - x) + 2y^2\delta)c_w^2 - (x\delta_-\delta_+ + 2y^2\delta)c_w^4]C_0(7) \\
& + y[y^2\delta^2(x-2\delta) + 2y(x^2\delta_+ - y(x\delta - 2\delta^2))c_w^2 - (x\delta_-\delta_+ + 2y^3\delta)c_w^4]C_0(8) \\
& + x[x^2\delta_x(3y^3 + \delta^2) + 2(x^2(y\delta_x + \delta^2) + y\delta(1-2x))c_w^2]C_0(9) \\
& + y\delta_y[y(x(3x^2 - \delta^2) + 2\delta^3) + 2(x(x^2 - \delta^2) + 2y\delta^2)c_w^2]C_0(10) \\
& - \delta^2[\delta(x\delta_-\delta_+ + 2y^2\delta) + 2(xy\delta_+ + 2y^2\delta)c_w^2]C_0(11)\} \\
& + \frac{m_Z^4}{2x^3y^2\delta^2}\{[3x^4y^3 + x^2y^2(-2\delta(y+3\delta) + x(5y+66) + 7x^2)c_w^2 \\
& + xy(6y\delta^2 + x(y(y-4\delta) - 2\delta^2) + 2x^2(3y+\delta) + 5x^3)c_w^4 + (x\delta_-\delta_+ + 2y^2\delta)c_w^6]D_0(4) \\
& + [(x\delta + \delta_+c_w^2)(x^3\delta^2 + 2x(x(x\delta_x + 3y^2) - 2y^2\delta_y))c_w^2 + (2y\delta_y + x(x^2 - 3y^2))c_w^4]D_0(5) \\
& + [y^2\delta^2(2\delta_y - 3x) + 2y(y\delta_y(2\delta_y - 5x) + x^3)c_w^2 + ((2\delta_y - y)y^2 - 3xy^2)c_w^4]D_0(6)\}, \tag{32}
\end{aligned}$$

$$A_6^l(x, y) = -A_4^l(x \leftrightarrow y), \tag{33}$$

$$A_7^l(x, y) = -A_5^l(x \leftrightarrow y), \tag{34}$$

$$\begin{aligned}
A_1^W(x, y) = & \frac{1}{2xy\delta_+}\{\delta_-[B_0(4) - B_0(3)] + \delta_+[x(B_0(1) - B_0(4)) - y(B_0(4) - B_0(2))]\} \\
& + \frac{m_Z^2}{4x^2y^2\delta}\{[\delta\delta_+(-x^2\delta + y^2(7x+y\delta)) - 2(\delta\delta_-(x^2+y^2) + 4xy\delta_+^2)c_w^2 - 2\delta_-\delta_+^2c_w^4]C_0(1) \\
& - \delta^2[x^2(x-\delta_y) + y^2(3x+\delta_y) + 2\delta_-\delta_+c_w^2]C_0(2) \\
& + x[x\delta(x\delta + 2y^2) - 2x(\delta_-\delta_+ + \delta_+^2)c_w^2 + \delta_-\delta_+c_w^4]C_0(3) \\
& - y[y^2\delta(5x+\delta_y) + 2y(\delta_-(1+\delta_-) - 4x^2)c_w^2 + \delta_-\delta_+c_w^4]C_0(4) \\
& - x[1-3y^2-\delta_+(2-\delta_+)-2(x+y(xy-\delta_y)-x^2(2-\delta_+))c_w^2]C_0(5) \\
& + y\delta_y[y\delta_y(2x+\delta_y) + 2(x-y\delta_y)c_w^2]C_0(6) \\
& + [-x(x+2\delta_y) + 2xy(x+2y)c_w^2 + \delta_-\delta_+c_w^4][xC_0(7) + yC_0(8)]\} \\
& + \frac{m_Z^4}{4x^2y^2\delta}\{[x\delta(3x(y-x\delta_x) + 2y(2x^2+y^2) - 13xy^2) + x^2\delta(x(1+x^2+y^2) \\
& + 2\delta_y(xy-\delta_-\delta_+))c_w^2 + x(\delta_+(y(2x+7y-3) - 3x\delta_x) + 8xy)c_w^4 + \delta_-\delta_+^2c_w^6]D_0(1) \\
& + [y^3\delta(x(4\delta_y-x) + \delta_y^2) + y^2\delta(3\delta_-(1+\delta_-) - 4xy)c_w^2 \\
& + y(x(x(x-7y)-2y) - 3\delta_-(x+y\delta_y))c_w^4 + \delta_-\delta_+^2c_w^6]D_0(2) \\
& + (xy-\delta_+c_w^2)[xy^2(x+2\delta_y) - 2xy(x+2y)c_w^2 - \delta_-\delta_+c_w^4]D_0(3)\}, \tag{35}
\end{aligned}$$

$$A_2^W(x, y) = -A_1^W(x \leftrightarrow y), \tag{36}$$

$$\begin{aligned}
A_3^W(x, y) = & \frac{1}{2xy\delta}\{B_0(3) - B_0(4) + 2x[B_0(4) - B_0(1)]\} \\
& + \frac{m_Z^2}{2x^2y^2\delta^2}\{-x^2\delta^2(\delta - 2c_w^2)C_0(2) + x[x\delta(x-\delta_+(x+2y)) + 2x(x\delta - 2y)c_w^2 - \delta_+^2]C_0(3) \\
& + \delta_+[x^2\delta(\delta_x - 5y) - 2x(x\delta - 2y)c_w^2 + \delta_+c_w^4]C_0(1) \\
& + x[x\delta_x(\delta_x(\delta - y) - 2y^2) - 2x(x+\delta^2)c_w^2]C_0(5)
\end{aligned}$$

$$\begin{aligned}
& + x[(xy(2(x\delta_x + y\delta_y) - xy) - 2xy(1 + \delta)c_w^2 - \delta_+^2 c_w^4]C_0(7)\} \\
& + \frac{m_Z^4}{2x^2 y^2 \delta^2} \{ -(xy - \delta_+ c_w^2)[xy(\frac{1}{2}xy + 2x\delta_x) - xy(1 + \delta)c_w^2 - x\delta_+ c_w^4]D_0(3) \\
& + [x^2 \delta^2(x\delta_x - y(3 - 2y)) + x\delta(5xy\delta_y + y(x^2 + 2y^2) + 3x^2 \delta_+)c_w^2 \\
& + x\delta_+(3x\delta_x - 2xy + y(y - 5))c_w^4 - \delta_+^3 c_w^6]D_0(1)\} \\
& + (x \leftrightarrow y),
\end{aligned} \tag{37}$$

$$\begin{aligned}
A_4^W(x, y) = & -\frac{2}{x\delta_+} + \frac{1}{x^2 \delta_y \delta_+^2} \{ 2(2x + y)[B_0(4) - B_0(3) + y(B_0(2) - B_0(4))] + x^2(B_0(2) - B_0(3)) \} \\
& + \frac{m_Z^2}{x^3 y \delta_y \delta^2} \{ -\delta_y[2y\delta_+ + 2\delta(x^2(\delta_- - 1) - y^2)c_w^2 + y\delta_+ \delta^2 c_w^4]C_0(1) + y\delta_y \delta^2(\delta - 2c_w^2)C_0(2) \\
& + x\delta_x c_w^2[x\delta(2y - \delta_x) + y c_w^2]C_0(3) + y\delta_x[y\delta^2 + \delta(x\delta_x + 2y)c_w^2 + y c_w^4]C_0(4) \\
& + x\delta_y \delta_x^3 c_w^2 C_0(5) - [y\delta \delta_y^2 - (\delta_y^2(2\delta_- \delta_+ + 2y\delta_x - x(1 + x^2)) + 2x^3 y^2)c_w^2]C_0(6) \\
& - y\delta_y(x\delta_y - c_w^2)c_w^2[xC_0(7) + 7C_0(8)] \} \\
& + \frac{m_Z^4}{x^3 y \delta^2} \{ c_w^2[x^2 \delta_x \delta^2 + x\delta(x\delta_x - y(2 - x))c_w^2 + y\delta_+ c_w^2]D_0(1) \\
& - [\delta_y^2 \delta^3 - y\delta^2(x(x - 2) + 3y)c_w^2 + \delta(x\delta_x \delta_- + 3y^2)c_w^4 - y\delta_+ c_w^6]D_0(2) \\
& + y(x\delta_x - c_w^2)(xy - \delta_+ c_w^2)c_w^2 D_0(3) \},
\end{aligned} \tag{38}$$

$$\begin{aligned}
A_5^W(x, y) = & \frac{2}{x\delta_+} + \frac{1}{x^2 y \delta \delta_+^2} \{ [\delta_+(y(3x - 2\delta_y) - x^2) - 2xy][B_0(3) - B_0(4)] \\
& + \delta_+^2[y(x - 2\delta_y)(B_0(4) - B_0(2)) + x^2(B_0(1) - B_0(4))] \} \\
& + \frac{m_Z^2}{2x^3 y^2 \delta_+ \delta^2} \{ \delta_+ \delta^2[\delta(x(x^2 + 5y^2) + 2y^2 \delta) - 2(x(x^2 + y^2) + 2y^2 \delta)c_w^2 \\
& - 2\delta_+^2(2\delta y^2 + x\delta_- \delta_+)c_w^4]C_0(1) \\
& + [\delta_+^2 \delta^2(x(x^2 + 5y^2) + 2y^2 \delta) - 2(x\delta_+ \delta_- + 2y^2 \delta)c_w^4 + 2\delta_+(\delta\delta_+(x^2 + 3y^2) \\
& + 2y(\delta^2(x^2 + y^2) - 2x^2 \delta_+))c_w^4]C_0(2) \\
& + x\delta_+[x^3 \delta^2 + 2x(-x\delta \delta_- + 2xy\delta_+ - y\delta)c_w^2 + (x\delta_- \delta_+ + 2y^2 \delta)c_w^4]C_0(3) \\
& + y\delta_+[y^2 \delta^2(5x + 2\delta) + 2y(2x^2 \delta_+ + \delta(x - 2\delta_x))c_w^2 + (x\delta_- \delta_+ + 2y^2 \delta)c_w^4]C_0(4) \\
& + x\delta_+[x^2 \delta_x(3y^2 - \delta^2) + 2(x^2(y\delta_x + \delta^2) - y\delta(2x - 1))c_w^2]C_0(5) \\
& + y\delta_+\delta_y[y(x(3x^3 - 5\delta^2) - 2\delta^3) + 2(x^3 - \delta_- \delta^2)c_w^2]C_0(6) \\
& + [-3x^3 y^2 + 2xy(2y(x - \delta) + x^2)c_w^2 + (x\delta_- \delta_+ + 2y^2 \delta)c_w^4][xC_0(7) + yC_0(8)] \} \\
& + \frac{M_Z^4}{2x^3 y^2 \delta^2} \{ [-x^4 \delta^3 + x^2 \delta(\delta(3x\delta_- + 2y(1 - 2y)) - 4xy\delta_-)c_w^2 \\
& + x(x\delta_+^2(4y - 3\delta) + 3\delta_- \delta_+ - x\delta + 2y\delta_x)c_w^4 + \delta_+(x\delta_- \delta_+ + 2y^2 \delta)c_w^6]D_0(1) \\
& + [-y^3 \delta^3(3x + 2y\delta) + y^2 \delta(4x^2 \delta_- \delta(x(5x - 3y + 4) - 6y))c_w^2 + (-3xy\delta(2x + y) \\
& + 2\delta^2(3y^2 - x\delta_-) + x^2(4(x^2 + y^2) + x(7y - \delta_x)))c_w^4]D_0(2) \\
& + (xy - c_w^2 \delta_+)[(3x^3 y^2 - 2xy(2y(2x - \delta_y) + x^2))c_w^2 \\
& + (x(3y^2 - x^2) - 2y^2 \delta_y)c_w^4]D_0(3) \},
\end{aligned} \tag{39}$$

$$A_6^W(x, y) = -A_4^W(x \leftrightarrow y), \tag{40}$$

$$A_7^W(x, y) = -A_5^W(x \leftrightarrow y), \tag{41}$$

with $B_0(i)$, $C_0(i)$, and $D_0(i)$ the two-, three- and four-point scalar functions given in the Appendix.

III. NUMERICAL RESULTS AND DISCUSSION

In the previous section the amplitudes for the sets of diagrams shown in Figs. 2–5 have been arranged in an $U_e(1)$ gauge invariant form. We have shown that the respective amplitudes are $SU(2)$ gauge independent and $U_e(1)$ gauge invariant for each set of diagrams in Figs. 2 and 3. This property enables us to discuss separately each contribution. In particular, we would like to study the role played by the off-shell $U_e(1)$ gauge structures of the Z boson and the neutrino. From (9) and (10) the double phase space integral for the decay width can be expressed as

$$\begin{aligned} \Gamma(Z \rightarrow \bar{\nu}\nu\gamma) = & \frac{m_Z}{256\pi^3} \int_0^1 dx \int_0^{1-x} dy \{ |\mathcal{M}_{Z^*}|^2 + |\mathcal{M}_{\nu^*}|^2 + |\mathcal{M}_{Box4}|^2 + |\mathcal{M}_{Box5}|^2 \\ & + 2\text{Re}[(\mathcal{M}_{\nu^*} + \mathcal{M}_{Box4} + \mathcal{M}_{Box5})\mathcal{M}_{Z^*}^\dagger + (\mathcal{M}_{Box4} + \mathcal{M}_{Box5})\mathcal{M}_{\nu^*}^\dagger \\ & + \mathcal{M}_{Box4}\mathcal{M}_{Box5}^\dagger] \}. \end{aligned} \quad (42)$$

In order to disentangle the relative importance of the contributions arising from the $ZZ^*\gamma$ and $\nu\nu^*\gamma$ couplings as well as the box diagrams, we have evaluated separately the corresponding terms in (42). In the case of the box diagrams contributions, we have obtained separately the contribution arising from each of the five $U_e(1)$ gauge structures defining these amplitudes. The result for the branching ratio $B(Z \rightarrow \bar{\nu}\nu\gamma)$ will follow immediately.

A calculation of this type requires a careful numerical evaluation of the Passarino–Veltman scalar functions, in particular of those arising from diagrams with resonant effects, as it is the case for the graphs shown in Fig. 4. Since some of the involved scalar functions can not be expressed in terms of elementary functions, it is necessary to evaluate them by means of more elaborated methods, such as the Fortran program FF [22]. We have made this task in different ways to get a reliable answer. In the case of the $ZZ^*\gamma$ and $\nu\nu^*\gamma$ couplings contributions, we get simple analytical solutions for the corresponding amplitudes, so we programmed the required integrals in Mathematica [23] and Fortran language together with the FF package. We have found an excellent agreement between the obtained results. In the case of the box diagrams, the four-point functions were analyzed by several methods. Explicit solutions of this functions were numerically evaluated and the results were compared with the corresponding evaluation using the FF package. In this way we are certain [24] that we get the correct answer for these functions. We found delicate cancellations arising from the box amplitudes and in order to get the required accuracy different integration methods were used.

Not all the box diagrams present troubles for their numerical evaluation. The most serious difficulties arise from the box diagrams shown in Fig. 4. In particular, the graphs (b) and (c) of this set induce collinear singularities. This fact implies, on one hand, that we must keep the lepton masses within the arguments of the scalar functions and, on the other hand, that we should have special care with the numerical evaluation of the corresponding amplitude. In order to get a reliable answer for these diagrams, we have used an entirely independent check. The idea is just to evaluate the amplitude via unitarity conditions

$$\text{Im}\mathcal{M}_{Box4} = \frac{1}{2} \int d\Phi_l \mathcal{M}(Z \rightarrow l^+l^-) \mathcal{M}^\dagger(\bar{\nu}\nu\gamma \rightarrow l^+l^-), \quad (43)$$

where $d\Phi_l$ is the phase space for the intermediate lepton pair. From the tree-level amplitudes of the right-hand side of this equation we can see that only the graphs 4(b) and 4(c) have collinear singularities. The result for the left-hand side of (43), obtained by the above described method, agrees nicely with the one obtained for the right-hand side.

We now proceed to discuss our results³. First, the $\nu\nu^*\gamma$ coupling contribution to the decay width $\Gamma(Z \rightarrow \bar{\nu}\nu\gamma)$ is 2.02×10^{-10} GeV. On the other hand, in the case of the $ZZ^*\gamma$ coupling only the top quark family gives an important contribution, namely 5.74×10^{-12} GeV, while the remaining contributions are negligible small. This fact can be understood because the $ZZ^*\gamma$ coupling contributions have a strong dependence on the mass gap existing in each fermion family. In particular, an exact mass degeneration implies a zero contribution. This nondecoupling effect of chiral fermions is well known in the SM and it is due to isospin breaking. This constitutes an important effect in radiative corrections proportional to $m_t^2 - m_b^2$. In the same footing, it is interesting to study a possible enhancement

³The values used for the SM parameters were taken from the Particle Data Group [25].

for the $ZZ^*\gamma$ amplitude arising from a fourth family of chiral fermions with SM assignment of quantum numbers. The most promising scenario arises from a heavy top-like quark with a light bottom-like quark and a light tau-like lepton. In order to give an estimation of this contribution, we have used the LEP1 lower bounds for the tau-like lepton and the bottom-like quark: $m'_\tau \leq 80$ GeV and $m'_b \leq 46$ GeV; also, a variation of m'_t in the 300–850 GeV range is assumed, where the upper limit for the top-like quark mass was taken from the $\Delta\rho$ constraint over the fourth family mass difference [26]. The corresponding contribution, as a function of $\Delta m = m'_t - m'_b$ shows an enhancement of almost 5 times with respect to the third family contribution, this enhancement is rapidly reached at $\Delta m = 300$ GeV. Finally, in the case of the box diagrams as well as the interference terms, their contribution is of the same order as that coming from the $\nu\nu^*\gamma$ coupling. We have found that the main contribution of the box diagrams arises from the $U_e(1)$ gauge structure corresponding to the neutrino MDT, whereas the $U_e(1)$ gauge structures given in (27) lead to a contribution of order 10^{-11} – 10^{-13} GeV.

In summary, considering all the terms in (42) and assuming lepton universality we have $B(Z \rightarrow \bar{\nu}\nu\gamma) = 7.16 \times 10^{-10}$ for the three SM neutrino species. The main contribution comes from the neutrino MDT $U_e(1)$ gauge structure, while the Z boson EDT contribution is two orders of magnitude below.

IV. FINAL REMARKS

We have presented a complete calculation of the SM decay $Z \rightarrow \bar{\nu}\nu\gamma$ using a nonlinear gauge. We have found that this decay is characterized by the off-shell electromagnetic properties of the neutrino and the Z boson: a neutrino MDT and a Z boson EDT induced by the $\nu\nu^*\gamma$ and the $ZZ^*\gamma$ couplings, respectively. We found that the Z boson EDT contribution may be enhanced by a fourth generation of chiral fermions; however, this effect is not enough to increase significantly $B(Z \rightarrow \bar{\nu}\nu\gamma)$. On the other hand, the main contribution to the decay $Z \rightarrow \bar{\nu}\nu\gamma$ arises from the neutrino MDT. This contribution depends strongly on the momentum transferred by the Z boson but it is not sensitive to a possible neutrino mass. Another interesting fact found in our calculation is that the box diagrams contributions can not be neglected because they induce a neutrino MDT $U_e(1)$ gauge structure with a form factor of the same order of magnitude as that coming from the $\nu\nu^*\gamma$ coupling. It is important to notice that this is true even though there is no $SU(2)$ nor $U_e(1)$ gauge link between the $\nu\nu^*\gamma$ and box diagrams. This scenario was foreseen in a recent study of the decay $Z \rightarrow \bar{\nu}\nu\gamma$ within the effective Lagrangian approach [8]: the operators inducing the $ZZ^*\gamma$ coupling are suppressed with respect to the dimension-six and dimension-eight operators inducing the $\nu\nu^*\gamma$ coupling and the box diagram contributions. Therefore, it is expected that the dimension-six and dimension-eight operators contribute substantially to $B(Z \rightarrow \bar{\nu}\nu\gamma)$, as it was the case in our calculation. Finally, we would like to point out that the decay $Z \rightarrow \bar{\nu}\nu\gamma$ leads to a branching ratio of the same order of magnitude than the one expected for the radiative decay $Z \rightarrow \gamma\gamma\gamma$ [27]. In this case, the experimental bound for the respective branching ratio is also about four orders of magnitude below the SM prediction. Therefore, these decay modes of the Z boson should be of interest for people searching for deviations coming from new physics effects.

ACKNOWLEDGMENTS

We appreciate useful discussions with J. L. Diaz-Cruz and F. Larios. MAP acknowledges the hospitality of the Aspen Center for Physics, where part of this work was done. Support from CONACYT (México) is acknowledged.

APPENDIX: PASSARINO–VELTMAN SCALAR FUNCTIONS

In this appendix we present the arguments of the scalar functions involved in the $Z\bar{\nu}\nu\gamma$ interaction. We follow the notation of [19] and the lepton mass was denoted by m_l .

Two-point scalar functions

$$\begin{aligned} B_0(1) &= B_0(xm_Z^2, m_l^2, m_W^2), \\ B_0(2) &= B_0(ym_Z^2, m_l^2, m_W^2), \end{aligned}$$

$$\begin{aligned}
B_0(3) &= B_0(m_Z^2, m_W^2, m_W^2), \\
B_0(4) &= B_0(\delta m_Z^2, m_W^2, m_W^2), \\
B_0(5) &= B_0(m_Z^2, m_l^2, m_l^2), \\
B_0(6) &= B_0(\delta m_Z^2, m_l^2, m_l^2).
\end{aligned} \tag{1}$$

Three-point scalar functions

$$\begin{aligned}
C_0(1) &= C_0(0, \delta m_Z^2, m_Z^2, m_W^2, m_W^2, m_W^2), \\
C_0(2) &= C_0(0, 0, \delta m_Z^2, m_W^2, m_l^2, m_W^2), \\
C_0(3) &= C_0(0, 0, x m_Z^2, m_W^2, m_W^2, m_l^2), \\
C_0(4) &= C_0(0, 0, y m_Z^2, m_W^2, m_W^2, m_l^2), \\
C_0(5) &= C_0(0, x m_Z^2, m_Z^2, m_W^2, m_l^2, m_W^2), \\
C_0(6) &= C_0(0, y m_Z^2, m_Z^2, m_W^2, m_l^2, m_W^2), \\
C_0(7) &= C_0(0, 0, x m_Z^2, m_W^2, m_l^2, m_l^2), \\
C_0(8) &= C_0(0, 0, y m_Z^2, m_W^2, m_l^2, m_l^2), \\
C_0(9) &= C_0(0, x m_Z^2, m_Z^2, m_l^2, m_W^2, m_l^2), \\
C_0(10) &= C_0(0, y m_Z^2, m_Z^2, m_l^2, m_W^2, m_l^2), \\
C_0(11) &= C_0(0, 0, \delta m_Z^2, m_l^2, m_W^2, m_l^2).
\end{aligned} \tag{2}$$

Four-point scalar functions

$$\begin{aligned}
D_0(1) &= D_0(0, 0, 0, m_Z^2, x m_Z^2, \delta m_Z^2, m_W^2, m_W^2, m_l^2, m_W^2), \\
D_0(2) &= D_0(0, 0, 0, m_Z^2, y m_Z^2, \delta m_Z^2, m_W^2, m_W^2, m_l^2, m_W^2), \\
D_0(3) &= D_0(0, 0, 0, m_Z^2, x m_Z^2, y m_Z^2, m_W^2, m_l^2, m_l^2, m_W^2), \\
D_0(4) &= D_0(0, 0, 0, m_Z^2, x m_Z^2, y m_Z^2, m_l^2, m_W^2, m_W^2, m_l^2), \\
D_0(5) &= D_0(0, 0, 0, m_Z^2, x m_Z^2, \delta m_Z^2, m_l^2, m_l^2, m_W^2, m_l^2), \\
D_0(6) &= D_0(0, 0, 0, m_Z^2, m_Z^2, \delta m_Z^2, m_l^2, m_W^2, m_l^2, m_l^2).
\end{aligned} \tag{3}$$

It is important to notice that lepton mass can be dropped out from the above equations, except in $C_0(7)$, $D_0(5)$ and $D_0(6)$, where collinear singularities arise.

-
- [1] M. Acciarri et al., L3 Collaboration, Phys. Lett. B412, 201 (1997); Phys. Lett. B346, 190 (1995).
 - [2] A. Barroso, F. Boudjema, J. Cole and N. Dombey, Z. Phys. C 28, 149 (1985).
 - [3] F. M. Renard, Nucl. Phys. B196, 93 (1982); D. W. Dusedeau and J. Wudka, Phys. Lett. B180, 290 (1986); U. Baur and E. L. Berger, Phys. Rev. D 47, 4889 (1993); D. Choudhury and S. D. Rindani, Phys. Lett. B335, 198 (1994); F. Boudjema et al., Phys. Lett. B240, 485 (1990).
 - [4] D. A. Dicus, S. Nandi and J. Woodside, Phys. Lett. B258, 231 (1991); J. Lopez, D. Nonapoulos and A. Zichichi, Phys. Rev. Lett. 77, 15168 (1998).
 - [5] T. M. Gould and I. Z. Rothstein, Phys. Lett. B33, 545 (1994).
 - [6] J. C. Romao, S. D. Rindani and J. W. F. Valle, Nucl. Phys. B443, 56 (1997).
 - [7] Y. Fukuda et al., Super-Kamiokande Collaboration, Phys. Rev. Lett. 81, 1562 (1998).
 - [8] M. Maya et al., Phys. Lett. B434, 354 (1998).
 - [9] M. Maltoni and M. I. Vysotsky, hep-ph/9804464 (unpublished).
 - [10] G. Degrossi, A. Sirlin and W. J. Marciano, Phys. Rev. D 39, 287 (1988).

- [11] J. L. Lucio Martínez, A. Rosado and A. Zepeda, Phys. Rev. D 29, 1539 (1984); Phys. Rev. D 31, 1091 (1985); N. M. Monyonko and J. H. Reid, Progr. of Theor. Phys. 73, 734 (1985).
- [12] A. Barroso, J. Pulido and J. C. Romao, Nucl. Phys. B267, 509 (1986).
- [13] K. Fujikawa, Phys. Rev. D 7, 393 (1993).
- [14] M. Baće and N. D. Hari Dass, Annals of Physics 94, 349 (1975).
- [15] N. M. Monyonko, J. H. Reid and A. Sen, Phys. Lett. B136, 265 (1984); N. M. Monyonko and J. H. Reid, Phys. Rev. D 32, 962 (1985).
- [16] F. Boudjema and E. Chopin, Z. Phys. C 73, 85 (1996).
- [17] U. Cotti, J. L. Diaz-Cruz and J. J. Toscano, Phys. Lett. B404, 308 (1997).
- [18] A. Abbasabadi, D. Bowser-Chao, D. A. Dicus and W. W. Repko, Phys. Rev. D 52, 3919 (1995).
- [19] R. Mertig, M. Böhm and A. Denner, Comp. Phys. Commun. 64 (1991) 345–359.
- [20] G. Passarino and M. Veltman, Nucl. Phys. 160B (1979) 151.
- [21] F. Boudjema and C. Hamzaoui, Phys. Rev. D 43, 3748 (1991).
- [22] G. J. van Oldenborgh, Comp. Phys. Commun. 66, 1 (1991).
- [23] S. Wolfram, Mathematica: A System for Doing Mathematics by Computer, Addison Wesley, 1992.
- [24] G. J. van Oldenborgh, private communication.
- [25] C. Caso et al., Review of Particle Physics, Eur. Phys. J. C3, 1 (1998).
- [26] J. F. Gunion, D. W. McKey and H. Pois, Phys. Lett B334, 339 (1994).
- [27] M. Yang and X. Zhou, Phys. Rev. D 52, 5018 (1995), and references therein.

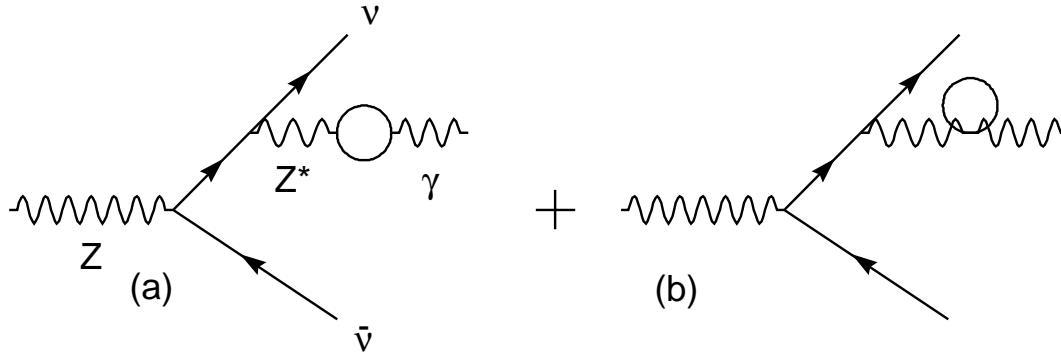


FIG. 1. $Z^* - \gamma$ mixing term. Its contribution vanishes in the nonlinear gauge.

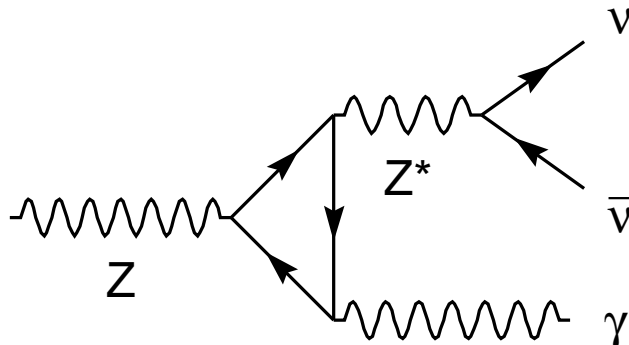


FIG. 2. $ZZ^*\gamma$ coupling contribution. The crossed diagram must be added.

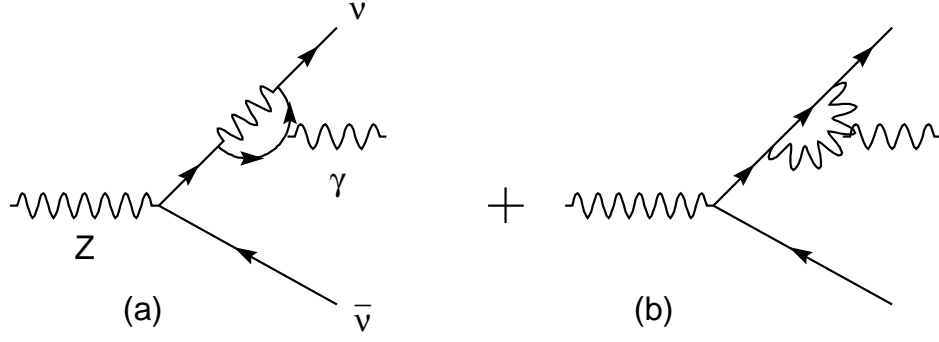


FIG. 3. $\nu\nu^*\gamma$ coupling contribution. The corresponding diagram with the loop in $\bar{\nu}$ must be added.

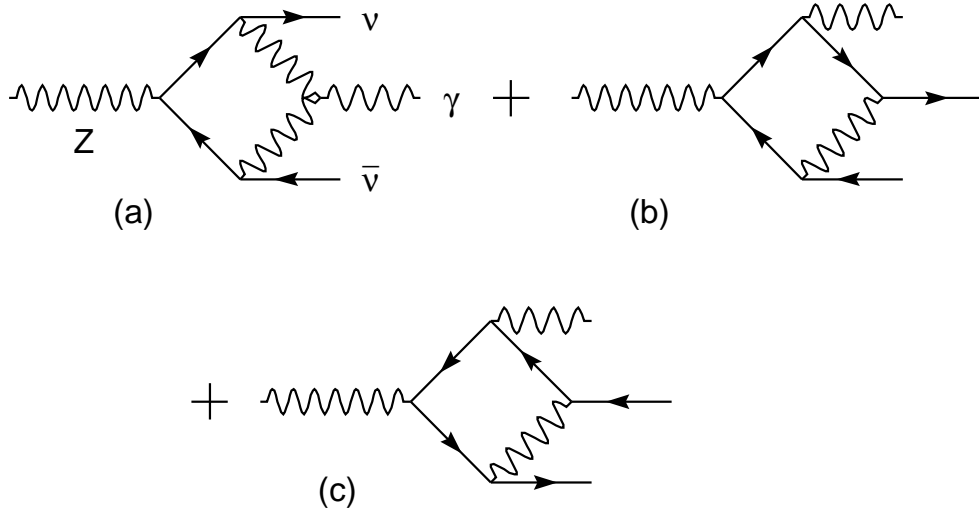


FIG. 4. Box diagrams with Zl^+l^- coupling.

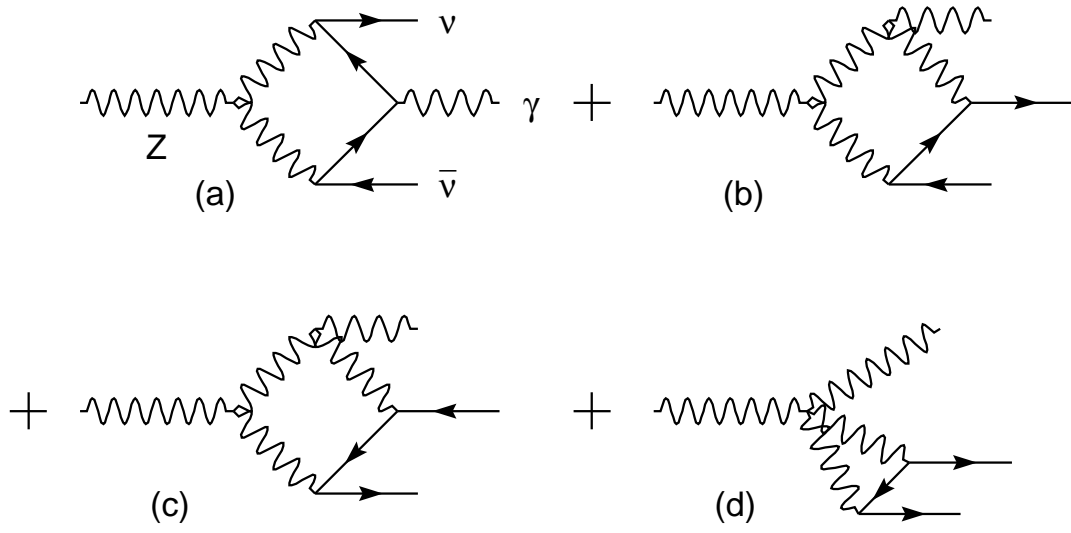


FIG. 5. Box diagrams with ZW^+W^- coupling.